

Automatic assessment of fuel load and fire risk via digitized database and intelligent computer vision

Yifei Ding^a, Rong Deng^a, Yuxin Zhang^{a,*}, Xinyan Huang^{a,*}, Negar Elhami-Khorasani^b, Thomas Gernay^c

^a Research Centre for Smart Urban Resilience and Firefighting, Department of Building Environment and Energy Engineering, The Hong Kong Polytechnic University, Hong Kong

^b Department of Civil, Structural and Environmental Engineering, University at Buffalo, Buffalo, NY, USA

^c Department of Civil and Systems Engineering, Johns Hopkins University, Baltimore, MD, USA

ARTICLE INFO

Keywords:

Fuel load
AI system
Deep learning
Smart firefighting
Web software
Fire risk

ABSTRACT

Fuel load assessment is essential to evaluate fire hazard and risk in fire engineering design for infrastructure, safety management, and firefighting operations. This study introduces an intelligent method to automatically assess indoor fuel load and fire safety by leveraging a digitized fuel load database and computer vision. First, a well-trained fuel recognition AI model automatically estimates the fuel load through image segmentation and classification. Next, fire hazard is predicted based on a parametric temperature-time model to evaluate fire safety and risk. The AI-aided assessment tool is open-access in a web application for free and real-time operation by feeding images from surveillance cameras and 360 panoramic cameras. A case study in an open office demonstrates the smart fuel load assessment achieving an agreement of above 94%, compared to the digitized survey method. Based on the AI-predicted fuel load, the estimated fire duration and maximum gas temperature are 32% and 13% higher, respectively, than the code-based assessments. Moreover, a fire risk heatmap is auto-generated to visualize the spatial distribution of high-load fuels and potential fire spread hazards. This automatic method enhances the accessibility, convenience, and cost-effectiveness of fuel load assessment while ensuring commendable accuracy. The application of this AI tool enables more accurate predictions of fire behavior, thereby supporting smart firefighting strategies and more effective emergency response.

Nomenclature Symbols

A	Area of surveyed room (m^2)
b	Side length of influence area in heatmap (m)
C_i	Color of influence area in the heatmap
H_i	Fuel load of each flammable item i (MJ/kg)
$H_{u,j}$	Net heat of combustion (MJ/kg)
h_{ij}	View transformation parameter
k	Form parameter
m_i	Mass of flammable item i (kg)
O	Opening factor
q	Fuel load density (MJ/m^2)
Q_i	Fire risk level of each fuel category
R_i	Standardized risk factor
R^2	Coefficient of determination

t	Time (hour)
α	Scale parameter
β	Position parameter
φ_j	Proportion of material j (%)
γ	Combustion factor
δ_{q1}	Fire activation risk factor due to compartment size
δ_{q2}	Fire activation risk factor due to compartment type
δ_{q3}	Factor considering active firefighting measures
Θ_g	Gas temperature in the compartment ($^{\circ}\text{C}$)

Abbreviations

AI	Artificial intelligence
APP	Application
GEV	Generalized extreme value distribution
HRR	Heat release rate
MSE	Mean square error

* Corresponding authors.

E-mail addresses: yx.zhang@polyu.edu.hk (Y. Zhang), xy.huang@polyu.edu.hk (X. Huang).

<https://doi.org/10.1016/j.psep.2025.107031>

Received 23 January 2025; Received in revised form 10 March 2025; Accepted 11 March 2025

Available online 13 March 2025

0957-5820/© 2025 The Author(s). Published by Elsevier Ltd on behalf of Institution of Chemical Engineers. This is an open access article under the CC BY-NC license (<http://creativecommons.org/licenses/by-nc/4.0/>).

PBD	Performance-based design
PTC	Parametric temperature curve
SD	Standard deviation

1. Introduction

Fuel load with a unit of megajoule (MJ) refers to the quantity of energy released by the complete combustion of all combustible material in a fire compartment (Fontana et al., 2016). Fuel load density refers to the quantity of combustibles per unit floor area, measured in MJ/m². Determining fuel load density in a compartment is the initial step of performance-based structural fire-resistance design and fire safety assessment (Shetty et al., 1998). It significantly affects the maximum gas temperature and fire development over time, along with other major factors like ventilation conditions (Zhang and Huang, 2024), compartment geometry, and thermal properties of compartment boundaries (Zhang et al., 2024a). Therefore, determining the fuel load is significant to estimating the appropriate design fires for structural fire design and assessment.

Structural design is increasingly shifting from prescriptive approaches to performance-based design (PBD), especially in cases where the design can be improved or optimized for safety and cost. In PBD, traditional code-based standard fire curves are replaced by natural fire curves (Gernay, 2019). Compared with the typical compartment fire curves, the parametric temperature-time curve (PTC) for structural fire design starts from the flashover and aims to estimate the temperature history only in the fully developed stage as the most dangerous period, because most structural failure occurs after the flashover (Ma and Mäkeläinen, 2000). Numerical fire models, such as computational fluid dynamics (CFD), are often too complex, and not suitable for light software packages that prioritize convenience for structural design purposes. Therefore, the parametric temperature-time curve offers a useful, simple, and convenient calculation procedure with a practical degree of accuracy, and is widely used in structural fire design (Ma and Mäkeläinen, 2000).

Fuel load density is one of the most important input parameters of PTC in structural fire safety assessment, and the determination of fuel load in a room is a relatively difficult task. For the structural design phase, that value is evaluated based on a deterministic value specific to the occupancy category provided by building codes and standards (National Fire Protection Association (NFPA) (NFPA), 2012; Institution,

2021; The Building Center of Japan, 2011; Her Excellency the Governor-General in Council, 2012). Statistics from numerous fuel load surveys are the basis for the fuel load design values in the codes and standards. Current fuel load survey methods include direct weighing (Caro and Milke, 1996), estimating from inventories (Kumar and Rao, 1997), a combination of weighing and inventory (Zalok and Eduful, 2013), use of questionnaires (Bwalya et al., 2004), and machine vision-based digitized method (Elhami-Khorasani et al., 2021a). The details of these methods are listed in Table 1. The direct weighing method (Caro and Milke, 1996) directly measures the mass of each fuel and calculates the total fuel load by multiplying the mass by the net heat calorific value of the composite materials. The inventory method (Kumar and Rao, 1997) estimates the mass of fuels by measuring their dimensions and calculating their volume. This volume is then multiplied by the density of the materials to determine the mass, using a similar item from catalogs as a reference. The questionnaire method (Bwalya et al., 2004) distributes survey sheets to room users, who provide information about the fuels present in their spaces. The common limitations of these methods include that the survey efficiency is low, and the size and fuel load of large items are not easy to measure. Therefore, simplifying and accelerating the measurement process is an urgent issue for high-efficiency and extensive fuel load data collection.

Onsite determination of fuel load density contributes to the fire safety and structural fire stability assessment of a compartment. The design values of fuel load density of a specific room category in codes and standards (National Fire Protection Association (NFPA) (NFPA), 2012; The Building Center of Japan, 2011; Her Excellency the Governor-General in Council, 2012) could be conservative or underestimated; for example, Eurocode (Institution, 2021) recommends using a fuel load of 80 % fractile. However, using such design values to infer temperature-time evolution induces error and may not reflect the true fire-resistance performance of the structure (Barnett, 2007). Therefore, for the fire safety assessment of a given compartment it is more reliable to use the onsite fuel load survey result of that specific compartment as the input for inferring the parametric temperature-time curve. In addition, efficient and accurate fuel surveying methods are needed to regularly evaluate and update code and standard values. Existing fuel load assessments are not efficient, making it challenging to support timely assessment of fire risk, structural fire resistance, and firefighting safety (Jadon and Kumar, 2025).

In recent years, artificial intelligence (AI) technologies based on big data, deep learning (DL) models, and computer vision (CV) algorithms are widely merged in fire safety engineering (Huang et al., 2022) e.g., fire detection (Liu et al., 2024), fire calorimetry (Wang et al., 2023a), prediction of temperature and smoke development (Kumari et al., 2021), fire critical events forecast (Zhang et al., 2024a, 2022a) and fire evacuation prediction and guidance (Zhang et al., 2024b; Ding et al., 2023). In particular, our previous work has studied how to use deep learning and CV algorithms to extract fire heat release rate (HRR) only from a fire image (Wang et al., 2023a, 2023b, 2022). In this study, we adopt deep learning and CV methods to train an AI model to conduct pixel-level image processing for fuel load recognition from fuel images. For example, the trained AI model could extract information from an onsite fuel photo to enable automatic detection (Zou et al., 2023) of fuels' location, instance segmentation (Liu et al., 2018) to eliminate the irrelevant background, and classification (Deng et al., 2009) of fuels' categories for matching corresponding calorific value and calculating fuel load. To develop the above AI engine, a fuel load database and a fitted CV-task deep learning model are indispensable for AI training.

This work aims to develop an AI-aided methodology to automatically identify fuel loads from room images for simplifying and accelerating the survey process and fire safety assessment. To this end, the paper makes the following contributions (Fig. 1):

Table 1
Comparison of fuel load measurement methods.

Method	Description	Pros	Cons
Direct weighing (Caro and Milke, 1996)	Direct measurement of the weight of the combustibles	Accurate	Infeasible and time-consuming
Inventory (Kumar and Rao, 1997)	Indirect estimation of the weight by measuring the dimension and the density of the fuels.	Acceptable Accuracy	Difficult and time-consuming
Questionnaire (Bwalya et al., 2004)	Distribution of questionnaires and estimation of the fuels through photographic selection and inventory tables.	Easy operation	Accuracy depends on subjective inputs, response rate/ completeness, and hard to verify.
Digitized survey (Elhami-Khorasani et al., 2021a)	Virtual measurement of fuel dimensions and accessing online inventory database to obtain weight and materials of fuels.	Moderately easy operation and accurate result	Time-consuming and hard to match in an online inventory database

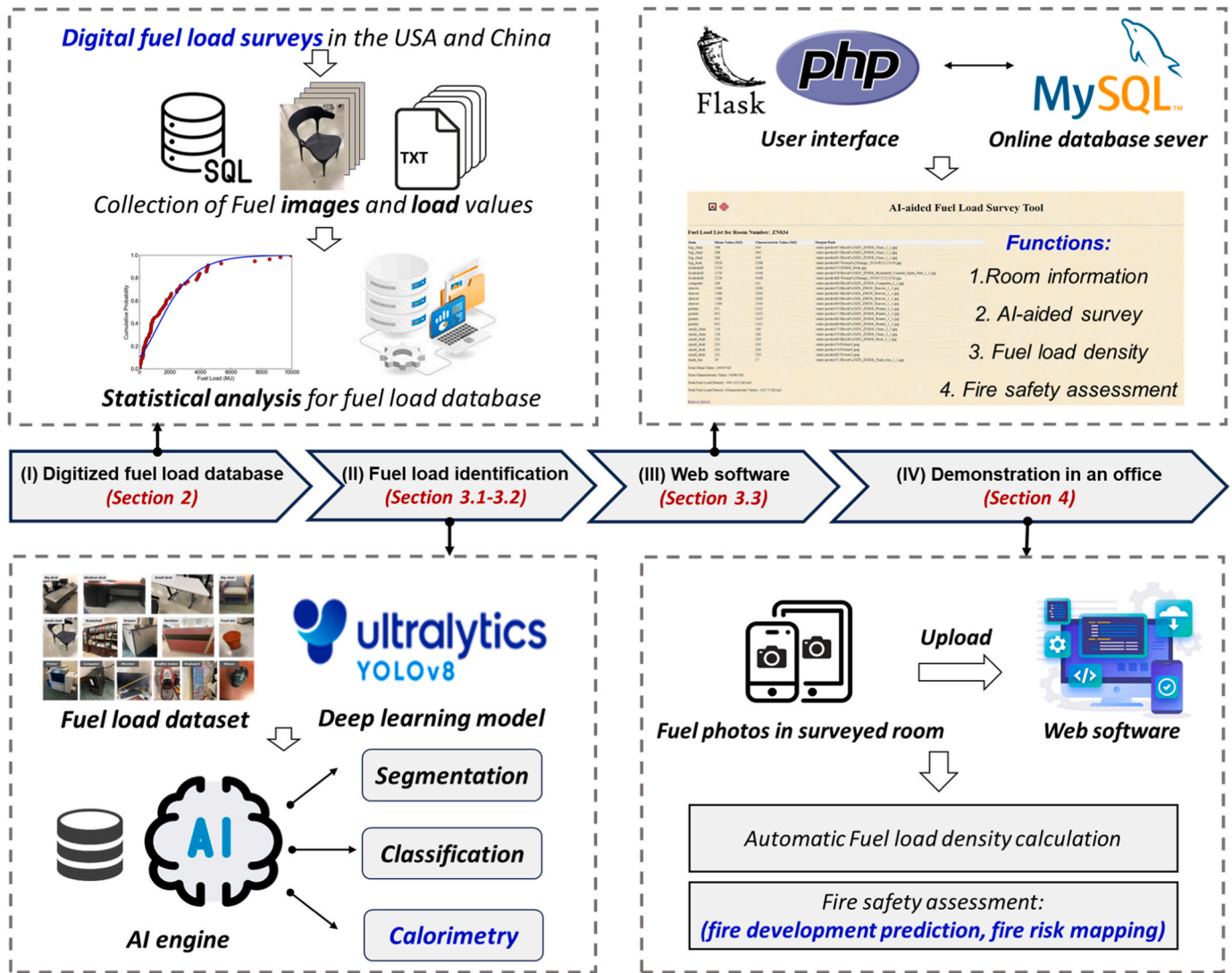


Fig. 1. Overall framework of this work.

- I. Expanding an existing digitized fuel load database by incorporating a comprehensive collection of images and fuel load labels for sorted fuels (Section 2).
- II. Training a fuel recognition deep learning model, incorporating fuel classification, detection, and segmentation using the proposed database. Additionally, a web software tool integrated with the pre-trained AI model and MySQL database is developed for rapid and convenient assessment of fuel load density and parametric temperature-time curve (Section 3).
- III. Demonstrating the methodology in an office compartment to validate the feasibility and convenience of fuel load measurement and fire safety assessment (Section 4).

2. Digitized fuel load database

2.1. Digitized data collection methodology

The collection of fuel load data derives from a series of fuel load surveys in the USA (46 rooms) and China (27 rooms) using the digitized survey methodology proposed by Elhami-Khorasani et al (Elhami-Khorasani et al., 2021a), as part of a project supported by the NFPA Fire Protection Research Foundation. The overall flowchart of the digitized survey method is shown in Fig. 2(a) with the major procedure consisting of the following steps:

- **Step 1 – onsite survey:** The surveyor takes snapshots of all potential fuel items and uses virtual measurement tools on a smartphone to determine their dimensions. Additionally, the surveyor needs to collect information about the room, including the layout, dimensions, and usage details.
- **Step 2 – match online inventory database:** The collected photos are uploaded to the online inventory engines (i.e., Google Lens <https://lens.google/> or Amazon Visual Search <https://www.amazon.com/visual-search>) to search for similar commodities with the surveying items and find their specifications to obtain the corresponding dimensions, mass, and material compositions.
- **Step 3 – calculate fuel load and data storage:** After the onsite survey, the collected data including the fuel item photos, dimensional measurements, and floor area of the room are uploaded to a dedicated survey application. This application then calculates the fuel load by multiplying the mass and material composition of each item by its corresponding calorific value by Eq. 1. The net heat of combustion of various typical materials (Elhami-Khorasani et al., 2019) is listed in Table A1 in Appendix. Finally, the surveyed data are stored in a structured online database by linking it to the SQL server.

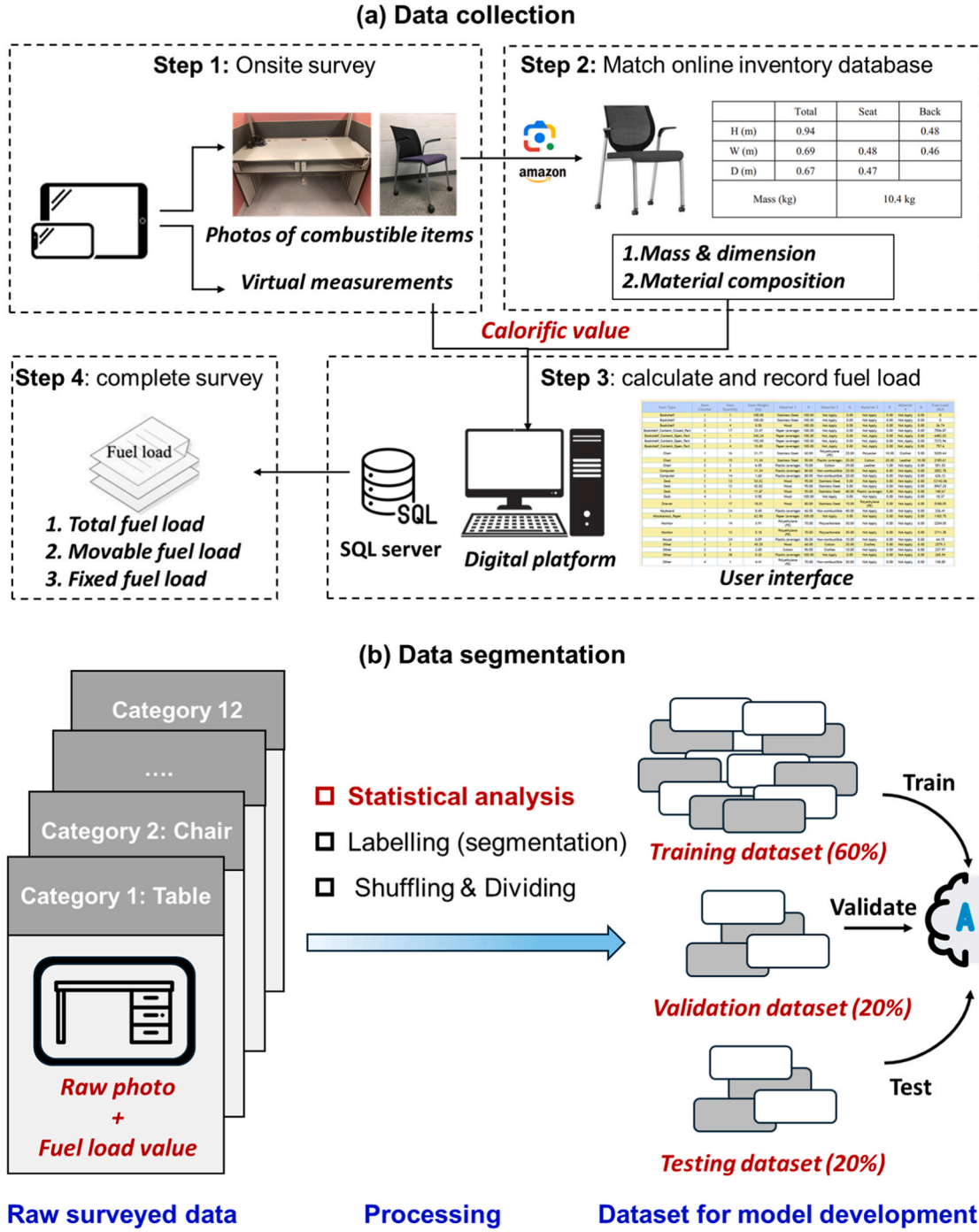


Fig. 2. Digitized fuel load database for AI model development (a) Flowchart of fuel load data collection using digitized survey methodology, (b) Procedure of fuel segmentation dataset for AI training.

$$H_i = \sum_{j=1}^n \varphi_j \bullet m_i \bullet H_{u,j} \quad (1)$$

$$q = \frac{\sum_i H_i}{A} \quad (2)$$

where, H_i – Fuel load of each flammable item (MJ), φ_j – Proportion of material j in the specific flammable item i (%), m_i – Mass of the flammable item i (kg), $H_{u,j}$ – Net heat of combustion or calorific value (MJ/kg), q – Fuel load density (MJ/m²), and A – Area of surveyed room (m²).

- **Step 4 – data visualization and analysis:** the surveyor obtains the total fuel load density by Eq. (2) for movable and fixed contents, and exports the data to conduct statistical analysis as required.

Using the above survey method, we investigated a total of 73 offices in different states of the USA, Mainland and Hong Kong of China, and collected over 1000 data-pair (raw photo and fuel load value) of common combustible furniture and electronic categories. As shown in Fig. 2 (b), the collected data-pair was conducted for further deep learning model development processing.

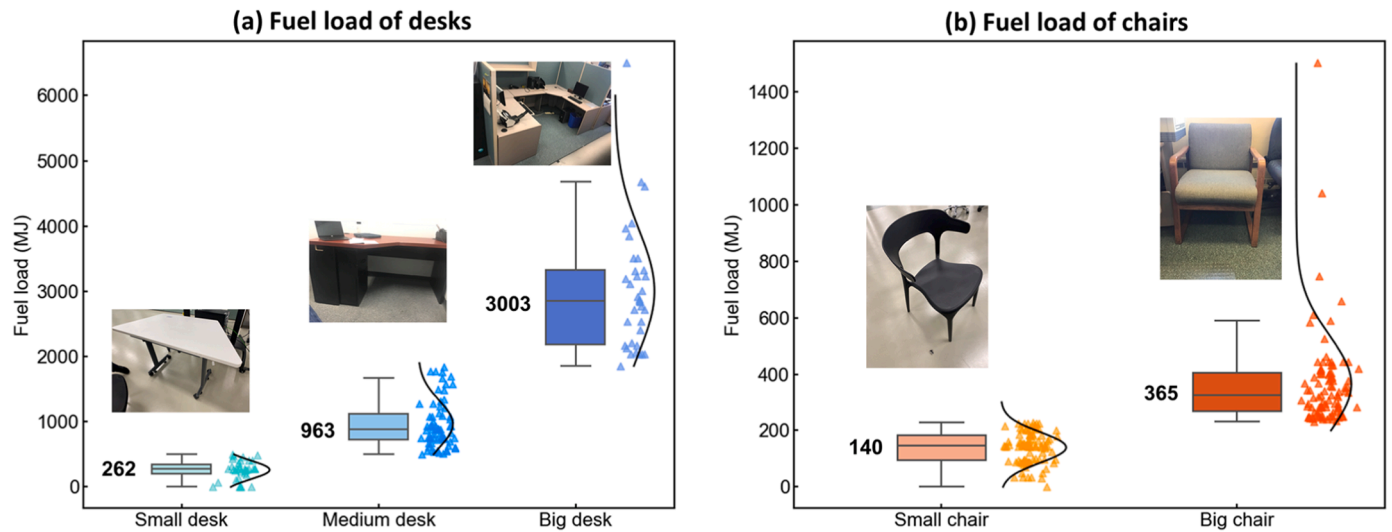


Fig. 3. Statistical distributions of fuel load values of surveyed desks and chairs.

Table 2

Summary of label values of fuel load (MJ) for different fuel types and corresponding image number.

Category	Type	Mean value μ (MJ)	STD σ (MJ)	Typical value q_k (MJ)	Number of images
Furniture	Big desk	3026	781	3588	44
	Medium desk	960	290	1169	33
	Big chair	368	100	440	156
	Bookshelf	476	367	740	130
	(empty)				
	Drawer	327	245	503	124
	(empty)				
	Partition	270	135	367	46
	Small desk	232	123	320	78
	Small chair	126	48	160	163
	Trash bin	40	25	57	61
	Bookshelf	2250	1637	3428	58
	content				
Electronic	Drawer	1262	743	1797	110
	content				
	Printer	955	656	1427	45
	Computer	306	146	411	31
	Monitor	213	108	291	91
	Coffee maker	38	27	57	21
	Keyboard	14.3	6.8	19.2	38
	Mouse	3.4	1.8	4.7	31

2.2. Preparation of fuel recognition dataset

Developing a deep learning model for fuel recognition containing segmentation, classification, and calorimetry of fuels requires a custom dataset with annotation labels. Fig. 2(b) illustrates the procedure from the raw digitized database to a fuel recognition dataset for AI training.

As shown in Fig. 2(b), the collected fuel data were categorized as 12 classes of common furniture (e.g., table, chair, bookshelf, drawer, etc.) and electronics (e.g., computer, monitor, printer, etc.) in the initial step. However, chairs and tables were found to be the most common movable fuels in modern compartments during the onsite surveys, and their dimensions differ a lot. To reduce the error induced by the dimensions of diverse chairs and desks, they were further categorized according to the observed shape features and size, shown in Fig. 3 and Fig. A1 in the Appendix. A common single desk no wider than 1.5 m and without drawers is categorized as a “Small desk.” A single desk combined with a drawer and a width over 1.5 m is regarded as a “Medium desk.” A large L-shaped or U-shaped office desk with a width of around 2 m is

categorized as a “Big desk.” Similarly, a light, small single chair made from plastic or with a small amount of cotton is classified as a “Small chair.” In contrast, a bigger chair with more wood, fabric, and cotton is classified as a “Big chair,” such as sofa chairs and big ergonomic chairs. Fig. 3 illustrates the statistical distributions of fuel load values for categorized desks and chairs, and different categories show distinct clusters of fuel load.

Moreover, the images of other common furniture and electronics in the surveyed offices were selected, cleaned, and shuffled in the dataset. Example images of all categories of common movable fuels are shown in Fig. A1. After annotation using the standard instance segmentation formats (Torralba et al., 2010) with a professional pattern recognition annotation tool, the dataset containing original images and corresponding label files (2D pixel coordinates of segmentation points) can be used to train, validate, and test the fuel recognition deep learning model.

2.3. Statistical analysis of representative fuel load values

In this section, statistical analysis was conducted to obtain representative fuel load values of different fuel categories, which would be used as the label value for fuel load identification. The fitted cumulative distributions of fuel load values for different fuel categories are shown in Fig. A2, where the Gumbel distribution function (Cooray, 2010) is used to fit the cumulative probabilities, which is the prescribed distribution for fuel load density in the Eurocode (Institution, 2021). The probability density function of Gumbel distribution (Cooray, 2010) is as Eq. (3):

$$f(x) = \alpha \exp\{-\alpha(x - \beta) - \exp[-\alpha(x - \beta)]\} \quad (3)$$

where α is the scale parameter, and β is the position parameter.

Moreover, the coefficient of determination (R^2) and mean squared error (MSE) are used as the metrics to show the fitting performance, calculated as Eqs. (4) and (5):

$$R^2 = 1 - \frac{\sum (Y_i - \hat{Y}_i)^2}{\sum (Y_i - \bar{Y}_i)^2} \quad (4)$$

$$MSE = \frac{1}{n} \sum_{i=1}^n (Y_i - \hat{Y}_i)^2 \quad (5)$$

where, n represents the number of samples, Y_i represents observed value (red scatter), \hat{Y}_i represents fitting value, \bar{Y}_i represents mean value of observed values.

The mean and standard deviation values of each fuel category are

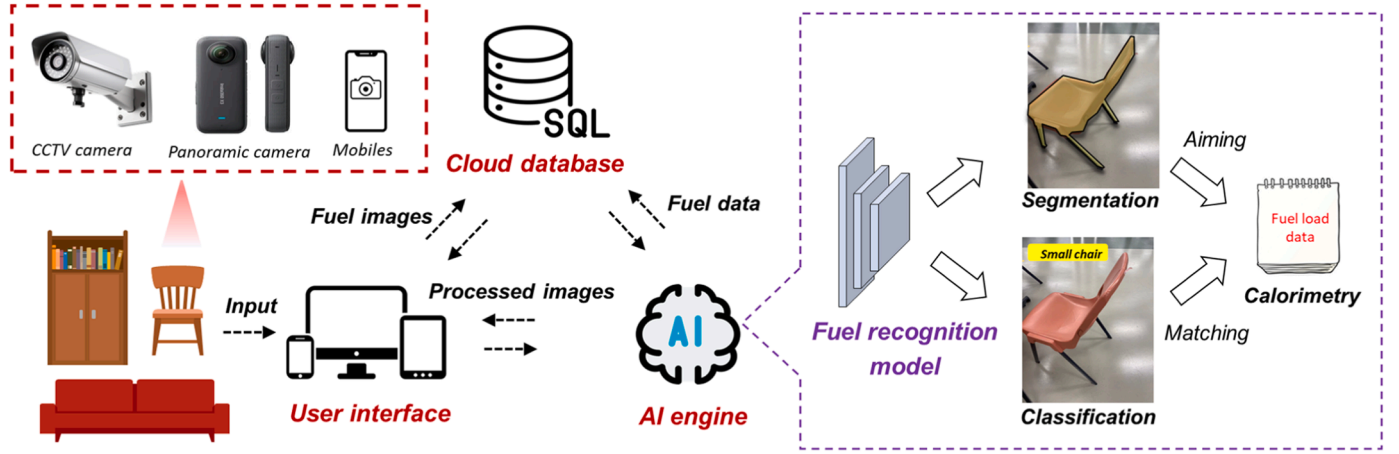


Fig. 4. Framework of proposed intelligent fuel load assessment method.

calculated from the fitting results in Eqs. (6) and (7), where $f(x)$ represents the function of the fitted curve. Moreover, the characteristic value of 80 % fractile of Gumbel distribution for each fuel category is calculated based on Eq. (8) (Fontana et al., 2016).

$$\mu = \sum_{i=1}^{\infty} x_i f(x_i) \quad (6)$$

$$\sigma = \sqrt{\sum_{i=1}^{\infty} (x_i - \mu)^2 \cdot f(x_i)} \quad (7)$$

$$q_k = 0.72 \cdot \mu + \sigma \quad (8)$$

where, μ is the mean value, σ is the standard deviation, q_k is the 80 % fractile value. The mean value and 80 % fractile values (typical value) are both used as the representative value of the fuel load of different fuel categories, which are listed in Table 2.

Miscellaneous paper, documents, and books in the drawers and bookshelf account for a major part of the total movable fuel load. Therefore, the statistics of fuel load value of drawer content and bookshelf content are analyzed and shown in Fig. A3. Gumbel distribution is also used to fit their cumulative distributions. Similar to other fuels, the representative values of bookshelf content and drawer content are calculated and listed in Table 2. For AI estimation, the total representative fuel load of the bookshelf or drawer equals to net fuel load (without content) plus the content.

3. Automatic assessment with AI computer vision

In this section, an automatic fuel load assessment method is proposed, which utilizes an image recognition model for the classification, instance segmentation, and calorimetry of fuels. As illustrated in Fig. 4, the framework of automatic fuel load assessment comprises a user interface, an AI engine, and a cloud database, which facilitates capturing and uploading fuel images, processing these images to estimate fuel load values, and storing all assessment data in a structured cloud spreadsheet. The integrated application includes uploading, processing, and analyzing photographs of fuels taken by diverse devices such as CCTV cameras, 360 panoramic cameras, and mobile portable devices. CCTV cameras can cover a wide area and reduce the assessment workload, but a single view angle may result in occlusion and omission of surveyed items. Panoramic cameras can cover almost all fuels in the survey room but may lead to severe distortion and recognition errors. The use of mobile devices to upload images with a single or small quantity of objects, while requiring more effort, provides the highest recognition accuracy. A case study is demonstrated in Section 4.

The embedded AI engine built on a fuel recognition deep learning model automatically processes the uploaded images using instance segmentation to identify the fuel object and its pixel location. Subsequently, the classification module recognizes the fuel category for further calorimetry. The calorimetry process matches the category of the fuels to a specific representative value derived from statistical analysis, and this value serves as the fuel load assessment result. Sections 3.2 and 3.3 will provide a detailed development process for the above fuel recognition model.

3.1. Computer vision and image database

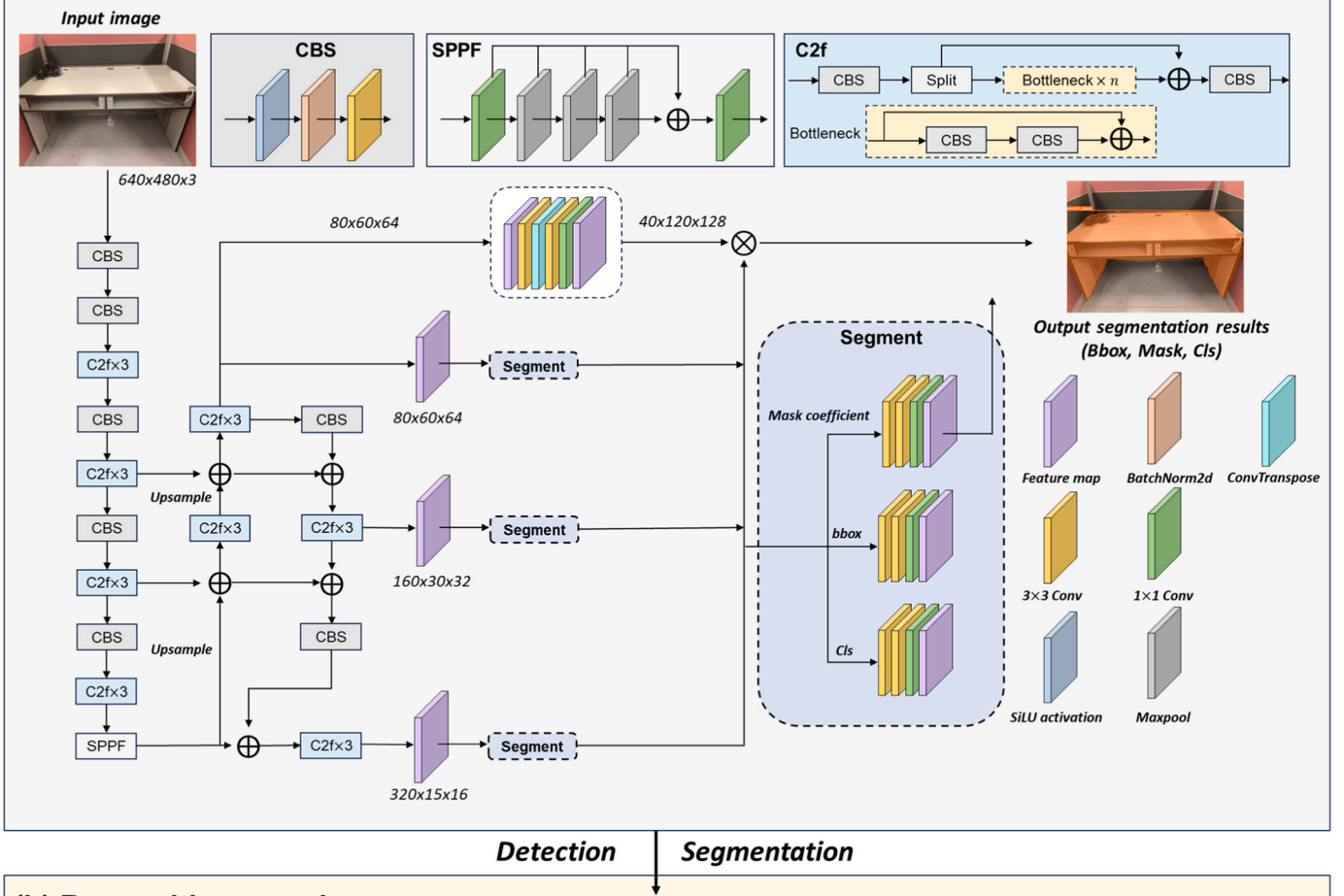
This section applies YOLOv8-seg (Ultralytics, 2023) as the fundamental model for fuel recognition (segmentation and classification). YOLOv8-seg is the instance segmentation sub-model of the YOLOv8 general structure, which enables the implementation of the computer vision tasks of image classification, object detection, and instance segmentation. Fig. 5(a) illustrates the architecture of YOLOv8-seg, which combines C2f module, CBS module, and SPPE module as the backbone, and employs PAN-FPN in the neck part for multilevel feature fusion for learning more information at various scales. The front-end segmentation head consists of three branches: regression of bounding box (Bbox), regression of mask segmentation, and classification. Therefore, the loss functions according to the above output tensors are DFL loss, CIOU loss, and Binary cross entropy loss, used for the refinements of segmentation mask boundaries, object detection Bbox, and classification, respectively (Li et al., 2023; Zhang et al., 2022a).

The images and annotations in the database were randomly disordered and then split into the training subset (659 images, 60%), the validation subset (213 images, 20%), and the test subset (213 images, 20%). The training set is utilized to train the model, the validation set is employed to assess the performance of the trained model during training, and the test set is utilized to measure the accuracy of object detection.

The training process is conducted on a desktop computer with the following configuration: NVIDIA GeForce RTX 4070, 12th Gen Intel(R) Core (TM) i5-12490F 3.00 GHz. The Pytorch (Paszke et al., 2019) is applied as the deep learning framework to build the model structure. During training, the batch size is set as 16, and the model is trained for a total of 300 epochs to ensure convergence. The training process is shown in Fig. A4. As the number of epochs increases, both the training loss and validation loss steadily decrease until reaching a very low value. This indicates that the model has converged and achieved a consistent and optimal performance.

Another metric to evaluate the training performance of the deep learning object detection model is the mean average precision (mAP)

(a) Architecture of fuel recognition



(b) Recognition samples

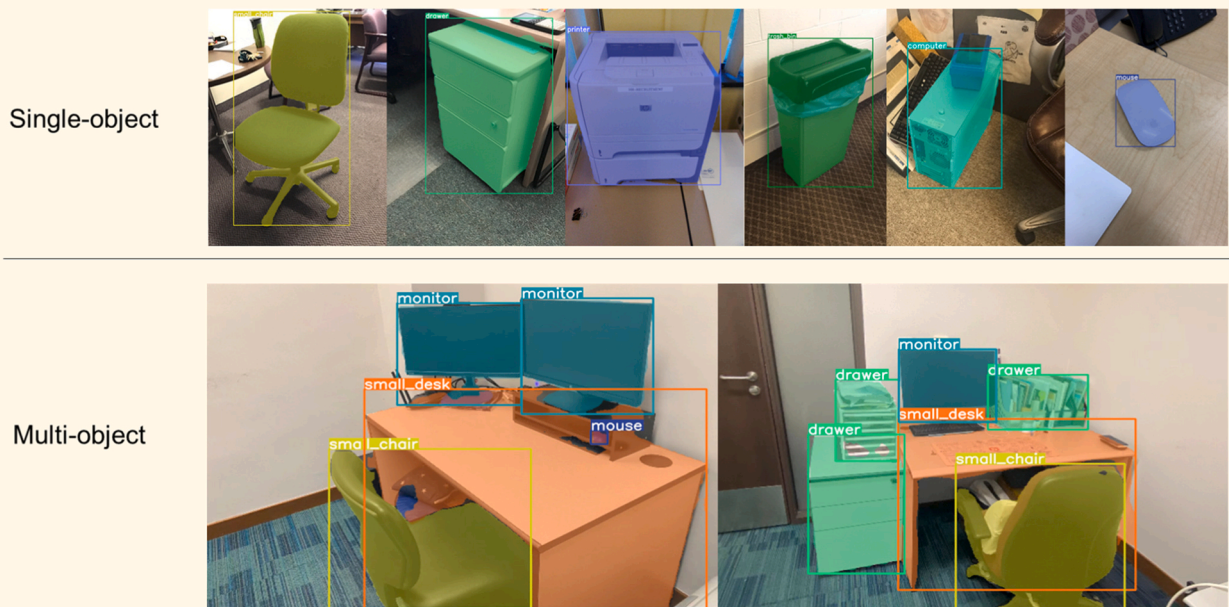


Fig. 5. Development of the fuel recognition model (a) YOLOv8-seg architecture for fuel segmentation and (b) Recognition samples from the testing dataset.

Table 3

Testing results of the segmentation model on the test dataset.

Class	Instance	Bbox				Mask			
		P	R	mAP50	mAP50-90	P	R	mAP50	mAP50-90
Big desk	9	0.62	0.89	0.83	0.65	0.62	0.89	0.83	0.51
Medium desk	6	0.23	0.33	0.18	0.18	0.23	0.33	0.18	0.15
Small desk	13	0.47	0.69	0.62	0.56	0.47	0.69	0.62	0.40
Big chair	29	0.82	0.87	0.86	0.81	0.81	0.86	0.86	0.78
Small chair	33	0.91	0.93	0.91	0.91	0.91	0.93	0.91	0.88
Bookshelf	18	0.8	0.89	0.85	0.75	0.8	0.89	0.85	0.78
Drawer	34	0.9	0.53	0.74	0.62	0.9	0.53	0.74	0.65
Partition	15	1	0.73	0.87	0.79	1	0.73	0.87	0.74
Trash bin	23	0.95	0.87	0.93	0.83	0.95	0.87	0.93	0.84
Printer	10	0.89	0.8	0.88	0.68	1	0.9	0.95	0.71
Computer	2	0.67	1	0.99	0.95	0.67	1	0.99	0.99
Coffee maker	4	0.8	1	0.95	0.79	0.8	1	0.95	0.71
Monitor	28	0.81	0.75	0.83	0.79	0.75	0.79	0.86	0.79
Keyboard	6	1	1	0.99	0.97	1	1	0.99	0.97
Mouse	2	1	1	0.95	0.93	1	0.98	0.96	0.94
Overall	213	0.72	0.75	0.76	0.69	0.73	0.76	0.77	0.66

(Zou et al., 2023). mAP is a comprehensive evaluation index combining Recall (R) and Precision (P), which eliminates the limitation of using a single metric. The average mAP curves of all classes in the training process are detailed in Fig. A4(b), in which the solid curve represents the mAP when the threshold equals 0.5 denoted as mAP @0.5, and the dash curve represents the average mAP in different thresholds ranging from 0.5 to 0.95 denoted as mAP @0.5:0.95. The mAP curves show that the prediction accuracy increases with the epochs and the average mAP of all classes after 300 training epochs achieved over 0.70.

After training, the models are evaluated on the testing dataset, which contains 213 images of 15 categories. The Recall (R), Precision (P), and mAP are used as the evaluation metrics, with the testing results shown in Table 3. The results show that the average mAP50 of Bbox and mask for all classes is over 0.76, and the average mAP50-90 also exceeds 0.67. Fig. 5(b) illustrates some examples of fuel load recognition results of each fuel category in the testing dataset. The reason for different classes achieving different mAPs can be related to the distinct attributes of each class. For example, highly accurate classes such as “electronics” have specialized characteristics that make them easier for the convolutional neural network to identify these attributes. In contrast, the “desk” class poses challenges due to the high similarity of features within its sub-categories. Therefore, more samples of diverse desks, especially “medium desk”, are required to be collected for the training dataset, and more advanced technologies and algorithms are needed to increase the recognition accuracy in future work.

3.2. Web software and user interface

The AI-aided software incorporating the proposed deep learning model is designed to assist fire engineers or any fuel load surveyors in conducting convenient and fast fuel load surveys and fire safety assessments. Fig. 6(a) illustrates the conceptual design of this AI-aided web software. The software contains four major sections, e.g., room information input, fuel recognition module, fuel load assessment page, and fire safety assessment page. The room information should be inputted by the surveyor manually, containing the length, width, and height of the room as well as the weighted average height and width of the room opening. All of these are crucial parameters for the fuel load density estimation and the fire development prediction.

The fuel recognition module, incorporating the pre-trained deep learning model, is the key section of the software responsible for segmentation, classification, and calorimetry from the uploaded photos. The fuel load assessment page is responsible for summarizing the survey list and calculating fuel load density. The fire safety assessment is based on the parametric temperature-time curve model (Institution, 2021) for compartment fire, facilitating the automatic calculation of maximum

gas temperature and fire duration, etc. All sections are interconnected via the background MySQL database (MySQL, 2001).

The website user interface is developed by PHP (Hypertext Preprocessor) (Welling and Thomson, 2003) and CSS (Cascading Style Sheet) (Meyer, 2006), and the backend is based on Python Flask and MySQL connector. Firstly, the user inputs the room information or selects a registered room to start a survey. After that, the user enters the panel of fuel recognition to upload the fuel photo shown in Fig. 6(b). After clicking the button “calculate”, the software calls the pre-trained deep learning model to process the image and display the instance segmentation, classification, and calorimetry results. The estimated fuel load results contain a “mean value” and a “characteristic value”. After uploading all fuel images, the user can click “check fuel load list” to enter the fuel load density assessment page, which displays a breakdown of all surveyed items, a summary of total fuel load, and calculated fuel load density. After that, users can enter the “Fire safety assessment page” (Fig. 6c) to check the potential fire development predictions. This page displays the critical calculation parameters, theoretical maximum temperature, theoretical fire duration and a figure of temperature-time-curve. A demonstration of the application operations is shown in Video S1 in Supplementary Material.

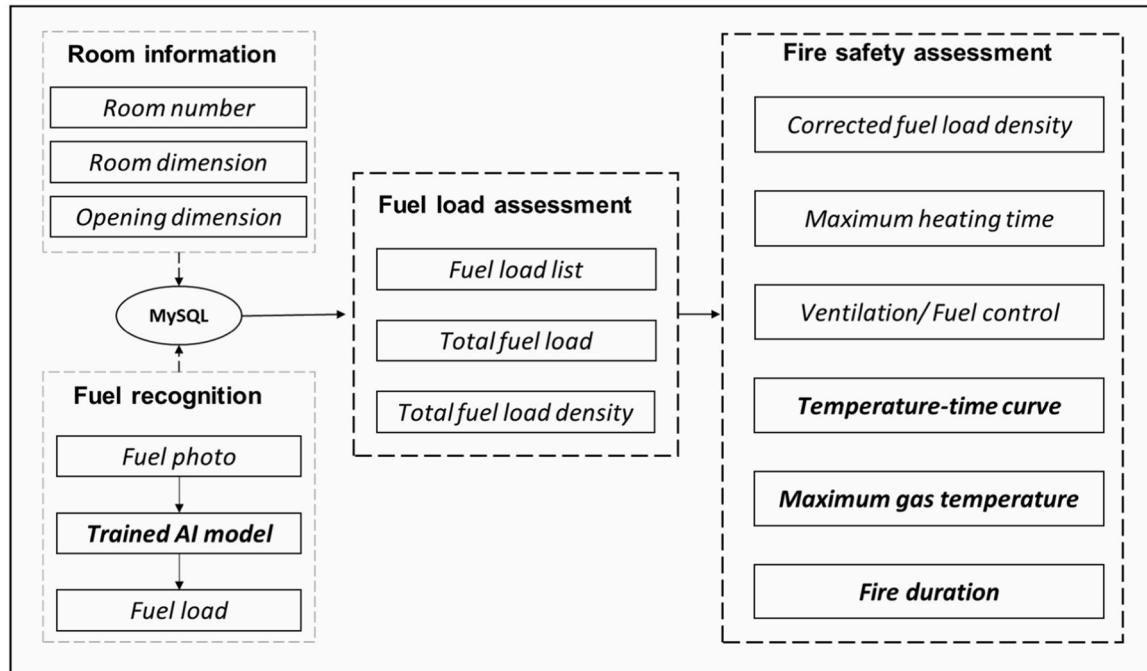
4. Demonstration in an office building

In this section, the developed AI-aided software will be used to assess the fuel load density and fire safety of an office compartment. The surveyed compartment is a large-space open office for research students. The total floor area is around 129 m² with a height of 3 m. The material of the ceiling and floor is concrete, and the enclosure material is brick. The office is equipped with automatic fire detection and sprinklers. Two data collection methods are used for comparison, namely individual image collection by mobile device and wide-view image collection by 360-degree panoramic camera.

4.1. Fuel load assessment by single images

The breakdown of the fuel load assessment of all fuels (over 300 items) in this compartment is listed in Table 4. The calculation results by the digitized survey method (Elhami-Khorasani et al., 2021a) serve as the reference data. The estimated total fuel load based on mean values from AI-aided software is 106,165 MJ, which approximates the ground-truth value (100,079 MJ). Fig. 7(a) shows discrepancies in all fuel assessment results between AI and the digitized method, where the average error is only 6.1%. In detail, when the fuel load is within 400 MJ, the errors for most fuels are within 15%. However, for items with very high true fuel loads (e.g., bookshelf), the error can be significant.

(a) Conceptual design of AI-aided web software




(b) Fuel recognition page

Working on Demo_room

Choose File No file chosen Calculate

Estimation Results:

- Fuel category: small_chair, Mean Value: 126 MJ, Characteristic Value: 160 MJ



[Back to choose room](#)

[Check fuel load list](#)

(c) Fire safety assessment page

Fire safety assessment of Demo_room (EN 1991-1-2 (2002))

Room Property

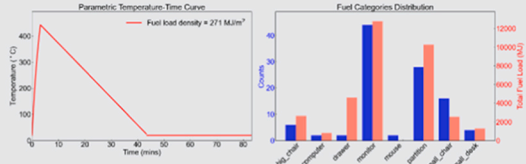
Room Length (m)	Room Width (m)	Room Height (m)	Floor Area (m ²)	Enclosure Area (m ²)	Weighted opening width (m)	Weighted opening height (m)	Ventilation Factor	Thermal Inertia
19.0	6.8	3.0	129.2	486.4	2.1	1.25	0.02	1699.6

Fire Safety Assessment

Corrected fuel load value (MJ/m ²)	Corrected fuel load related surface area (MJ/m ²)	Maximum heating time (hr)	Maximum heating time (min)	Maximum heating time* (hr)	Maximum heating time* (min)	Fire type
170.5	45.29	0.45	27.17	0.05	3.16	ventilation control

Maximum Gas Temperature: 443.5 °C

Fire Development & Fuel Load Distribution



[Back to Survey](#)

Fig. 6. (a) Conceptual design of AI-aided web software, (b) fuel recognition page of the software, and (c) fire safety assessment page of the software.

Although individual sample errors may occasionally be substantial, the overall assessment results can converge toward the statistical average and achieve a satisfactory error level when these errors are balanced by compensating errors across multiple items as the sample size increases. The overall fuel load density estimated by the AI method is 822 MJ/m², compared to 775 MJ/m² calculated by the digitalized method. Moreover, the AI method also provides the characteristic value (80% fractile)

of fuel load density, that is 1197 MJ/m², which can be used to calculate the parametric temperature-time curve.

Table 5 compares the digitized survey method and our proposed AI-aided fuel load assessment method. The digitized method involves using digital measurement apps on mobile devices to measure the dimensions of fuels and uploading photos to an online inventory database for matching similar products to obtain mass and material composition,

Table 4

Breakdown of fuel load survey results by digitized method and AI-aided method for the case study.

Category	Num	H (Dig.) [MJ]	H_i (Dig.) [MJ]	H (AI) [MJ]	H_i (AI) [MJ]	Typical value (80% fractile) [MJ]
Bookshelf	1	3636	3636	2726	2726	4168
Bookshelf	1	6482	6482	2726	2726	4168
Chair	27	3934	146	3402	126	4320
Chair	3	552	184	378	126	480
Chair	16	5201	325	5888	368	7040
Computer	21	939	44.7	6426	306	8631
Computer	16	5072	317	4896	306	6576
Desk	1	141	141	232	232	320
Desk	37	27,650	747	8584	232	11,840
Desk	4	3736	934	928	232	1280
Drawer	23	17,243	750	36,547	1589	52,900
Keyboard	37	349	9.4	529	14.3	710
Monitor	20	3149	157	4620	231	5820
Monitor	26	5423	209	6006	231	7566
Mouse	37	99	2.7	126	3.4	174
Partition	48	9513	198	12,960	270	17,616
Partition	23	5701	248	6210	270	8441
Printer	1	192	192	955	955	4127
Printer	2	1012.1	506	1910	955	8254
Trash bin	3	52	17.5	116	38.8	170
Total fuel load		100,079		106,165		154,601
FL density [MJ/ m²]		774		822		1197

shown as Section 2.1. Both onsite dimension measurement and offsite online queries are time-consuming and labor-intensive, typically requiring over 40 minutes to complete a fuel load assessment task for a single standard office. In comparison, using the AI-aided method could significantly improve automation and reduce workload. The survey tool and procedure are much simpler because engineers only take some time to take onsite snapshots and upload them to the incorporated software, and the AI engine can finish all fuel load estimation in a few seconds. If considering the digitized fuel load assessment result as the reference value, the AI assessment method achieves an error margin within 10%, demonstrating satisfactory accuracy. While our comparisons demonstrate strong agreement, we recognize the need for further validation using more accurate measurement method, such as direct burning test of a combustible item by measuring heat release and mass loss.

4.2. Fuel load assessment by panoramic camera

Although utilizing a single camera input for AI-based fuel load assessment achieves satisfactory accuracy, it still necessitates taking and

uploading a large number of photos, which could be a significant workload. To address this issue, a 360-degree panoramic camera is employed, enabling capturing two wide-view images in a single shot in Fig. 8(a). For comparison, Fig. 8(b) shows the fuel load recognition using the two wide-view images derived from the panoramic image to address the distortion issue, where most fuels are accurately identified.

Object occlusion remains a challenge when using panoramic cameras, as depth field compression can lead to an underestimation of the total predicted fuel load compared to the true value. For instance, partitions in an open office space can be easily detected, but often block the view of other fuels, such as desks and chairs. To address this issue, we propose estimating the total fuel load based on the detected partitions. This method assumes that all partitions are fully identified and there is a linear correlation between the fuel load of the partitions and the overall fuel load in the office. Fig. 7(b) illustrates the relationship between the fuel load of partitions and the total fuel load, accompanied by a linear fitting curve. Data from 9 small offices and 2 large open offices with partitions in the digitized fuel load database are analyzed. The linear correlation between partition's fuel load (Q_p) and total fuel load (Q_t) denotes as

$$Q_t = 11(Q_p + 2,000) \text{ [MJ]} \quad (9)$$

where the unit of Q is MJ, and the fitting coefficient is $R^2 = 0.83$.

In this office, the AI-based fuel load assessment of all partitions from the panoramic image is 6480 MJ. Using Eq. (9), the predicted total fuel load for this room is calculated to be 93,280 MJ. Consequently, the

Table 5

Comparison of previous digitized survey method (Barnett, 2007) and proposed automated AI-aided method.

Features	Digitized survey method (Elhami-Khorasani et al., 2021; Ding et al., 2024)	Automatic AI-aided method (single images)	Automatic AI-aided method (panoramic images)
Survey Tool	Camera + rangefinder + online inventory database	Camera + AI interface	Panoramic camera + AI interface
Method complexity	High	Low	Very low
Workload	High	Low	Very low
Time of onsite survey	10 min – 30 min	< 10 min	< 3 min
Time of fuel load estimation	> 10 min	Seconds	Seconds
Accuracy of results	Reference value	> 90%	> 90% after correction

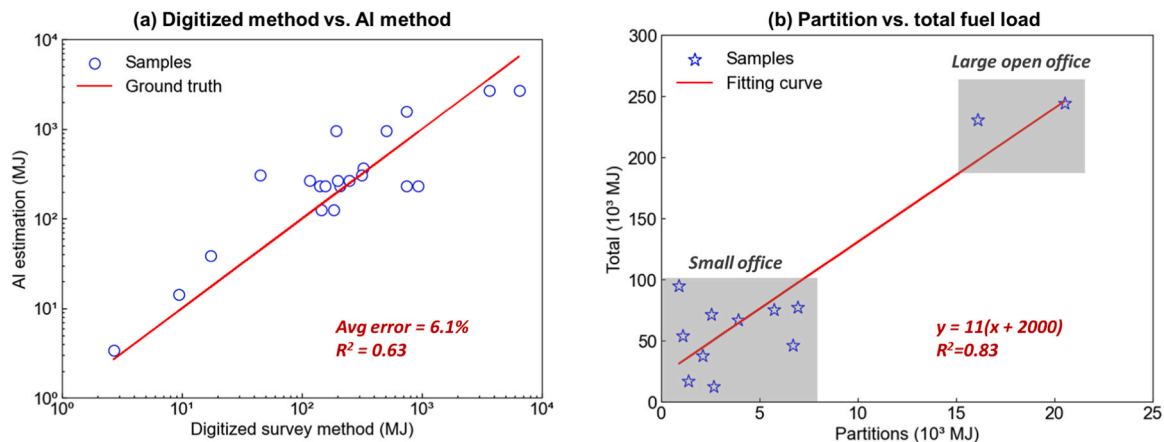


Fig. 7. (a) Fuel load assessment result of all fuels in the office compartment, and (b) Fitting curve of relationship between fuel load of partitions and total value.

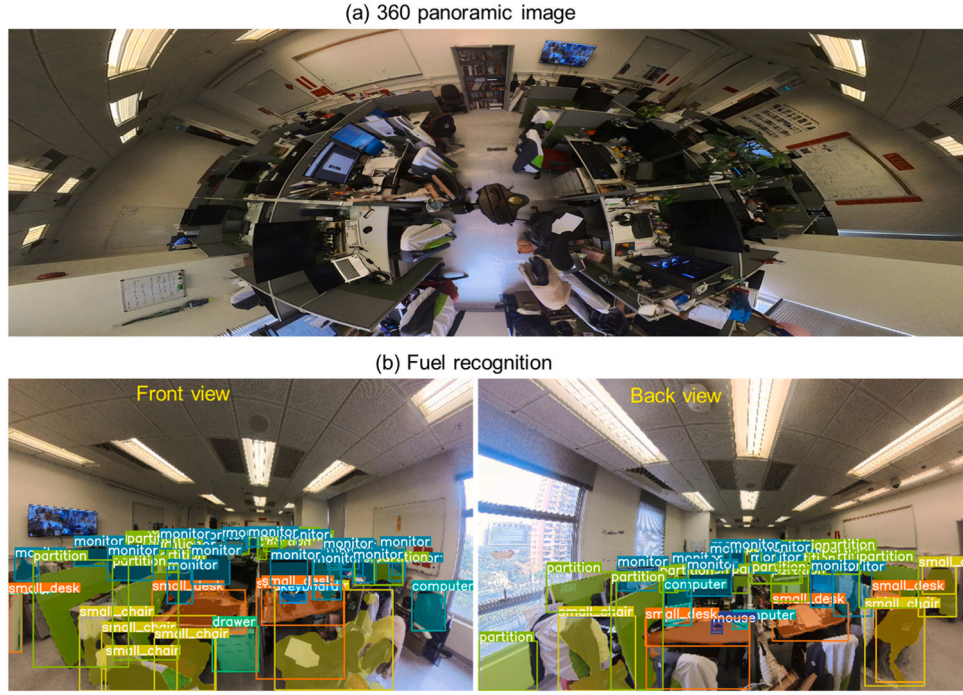


Fig. 8. (a) A 360 photo of the demonstrated office, and (b) the fuel recognition results from the wide-view images (derived from the 360 photo) by the panoramic camera.

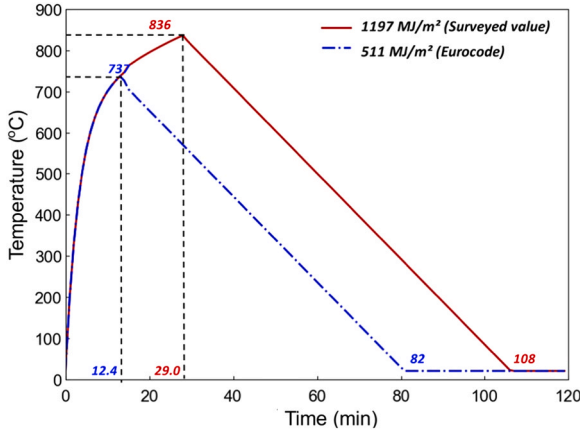


Fig. 9. Comparison of parametric temperature-time curve.

agreement between the AI assessment and the true value is 93.2%, which demonstrates satisfactory accuracy with enhanced efficiency of the fuel load assessment process. Even though, the validity and accuracy of the correlation between partitions and total fuel load in the office room require further validation through additional case studies in future work. Table 5 compares the AI estimations between single images and 360 panoramic images. The latter method is much more convenient, faster, and easier to operate. However, the prediction accuracy is affected by object occlusions, but it could achieve an acceptable estimation after correction with partitions' fuel load.

This case demonstrates the promising capabilities of the proposed AI-aided method for automatic assessment of fuel load density in an office environment. The results indicate a close approximation between the AI estimation and the previously digitized method with a satisfactory level of accuracy, and the AI-aided method achieves a significant reduction in time and labor. However, the proposed AI method is also subject to the problem of data dependency, as its performance relies heavily on the quality, quantity, and diversity of the training data.

4.3. Application to fire development evaluation

The fire safety assessment module embedded in the developed software is based on an empirical model of parametric temperature-time curve in Eurocode (Institution, 2021; Dundar and Selamet, 2023; Khorasani et al., 2014) as:

$$\Theta_g = 20 + 1325(1 - 0.324e^{-0.2t^*} - 0.204e^{-1.7t^*} - 0.472e^{-19t^*}) \quad (10)$$

where Θ_g is gas temperature in the compartment, t^* is time multiplies by a function of opening factor and boundary thermal properties. The maximum gas temperature occurs when:

$$t_{\max} = \max(0.2 \times 10^{-3} q_{t,d} / O; t_{\lim}) \quad (11)$$

where O is the opening factor: $A_v \sqrt{h_{eq}} / A_t$, A_v is total area of vertical openings, h_{eq} is weighted average of window heights; t_{\lim} is 20 mins for office (medium fire growth rate), $q_{t,d}$ is the design value of fuel load density related to the total enclosure boundary area A_t and floor area A_f , whereby:

$$q_{t,d} = q_{f,d} \bullet A_f / A_t \quad (12)$$

where $q_{f,d}$ is the design value of the fuel load density, whereby:

$$q_{f,d} = q_{f,k} \bullet \gamma \bullet \delta_{q1} \bullet \delta_{q2} \bullet \delta_{q3} \quad (13)$$

where $q_{f,k}$ is the characteristic value of the fuel load density. In this case, the characteristic value estimated by AI equals to 1197 MJ/m². In Eurocode, $q_{f,k}$ of office category equals to 511 MJ/m². γ is the combustion factor, assumed as 0.8 for mainly cellulosic materials. δ_{q1} is a fire activation risk factor due to compartment size, assumed as 1.29 in this case. δ_{q1} is a fire activation risk factor due to compartment type, which is 1.0 for offices. δ_{q3} is a factor considering active firefighting measures, which assumed as 0.61 in this case. The gas temperature during decay phase is calculated by,

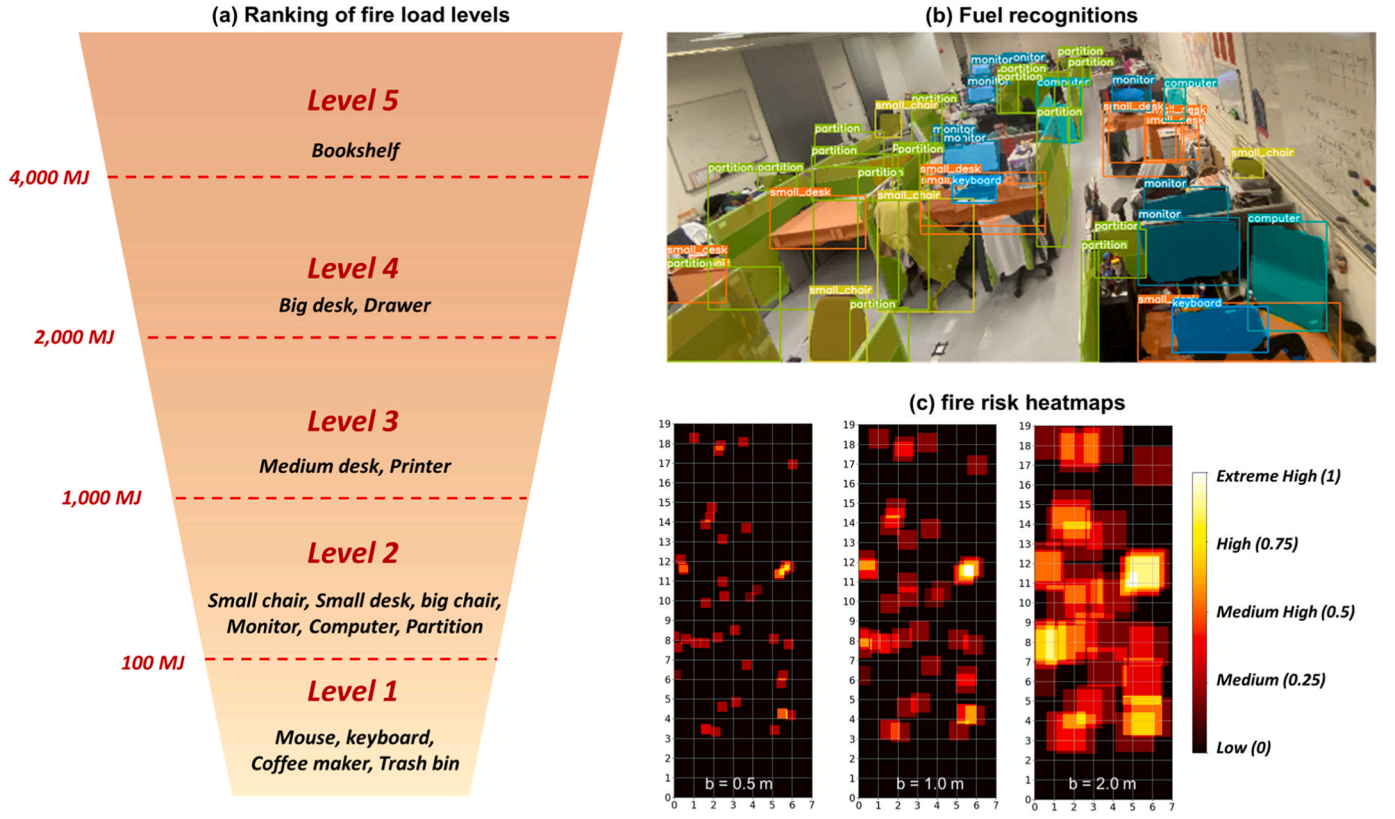


Fig. 10. (a) Five levels of indoor combustible fuel loads, (b) fuel load identification demonstrated in office, and (c) fire risk heatmaps under different influence areas of $b = 0.5$ m, 1.0 m, and 2.0 m.

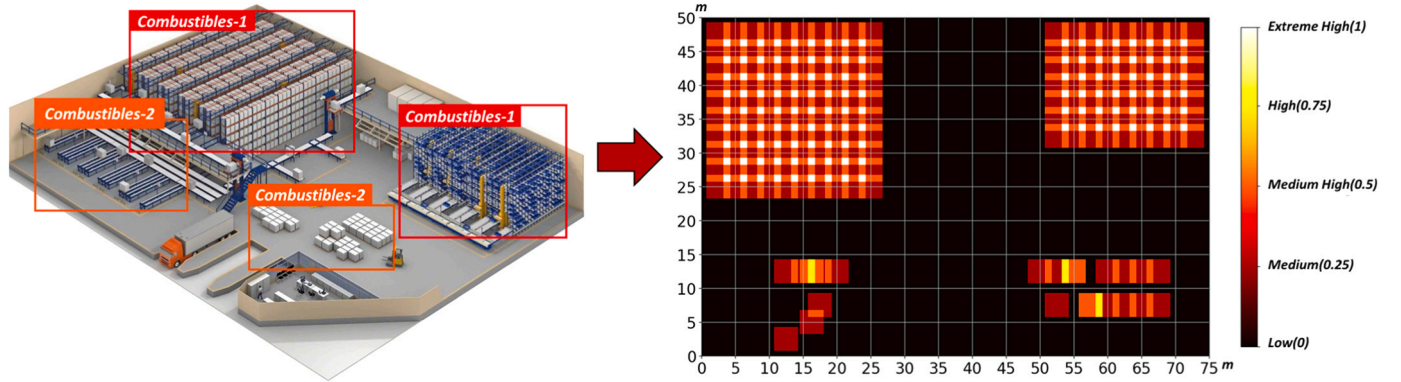


Fig. 11. Illustration of potential application of the proposed method for fire risk monitoring of a warehouse.

$$\theta_g = \begin{cases} \theta_{\max} - 625(t^* - t_{\max}^* \cdot x), & t_{\max}^* \leq 0.5h \\ \theta_{\max} - 250(3 - t_{\max}^*)(t^* - t_{\max}^* \cdot x), & 0.5h \leq t_{\max}^* \leq 2h \\ \theta_{\max} - 250(t^* - t_{\max}^* \cdot x), & t_{\max}^* \leq 2h \end{cases} \quad (14)$$

where, x is parameter related to t_{\max} and t_{\lim} . In this case, $t_{\max} > t_{\lim}$, so $x = 1.0$.

According to the above model, the developed software outputs the fire safety assessment results for this office compartment, shown as a red curve in Fig. 9. The maximum heating time is 29.0 minutes resulting in the maximum gas temperature of 836 °C. The decay phase lasts over 75 minutes, gradually decreasing to the ambient temperature (20 °C), resulting in an overall fire duration of 108 minutes. In comparison, the blue dashed curve shows the estimation result using Eurocode design value (511 MJ/m²). The maximum gas temperature is 737 °C, and

heating time lasts 12.4 minutes. The overall fire duration is 82 minutes. The underestimation of heating time and fire duration compared to the assessment with the actual fuel load density could lead to incorrect judgments by firefighters regarding critical moments and the optimal rescue duration during firefighting operations in fire scenarios.

A comparison of fire scenario prediction between fuel load design value and on-site estimated value shows that reliance on code-based evaluations may inadvertently underestimate real fire risks, potentially compromising safety measures. While code-based assessments such as those outlined in the Eurocode, provide a standardized framework for fire safety, they must rely on generalized assumptions of fuel load design value that may not accurately reflect the conditions of a specific building. With advances in technology and data processing capabilities, there is an opportunity for a refined estimate of the actual fuel load and fire risk in each building compartment at any given time. The

Table A1

List of net heat of combustion (calorific value) of different materials for fuel load calculation.

Material	Calorific value (MJ/kg)	Material	Calorific value (MJ/kg)
Acrylonitrile-Butadiene-Styrene (ABS)	36.4	Polyester	26.9
Celluloid	18.5	Polyethylene (PE)	45.0
Cellulose	18.1	Polyisocyanurate foam	24.3
Cellulose triacetate	18.4	Polymethylmethacrylate (PMMA)	24.6
Clothes	20.2	Polypropylene	44.1
Cork	29.2	Polystyrene	40.6
Cotton	19.8	Polyurethane	26.7
Kerosene	41.2	Polyvinylidene chloride	17.1
Leather	19.0	Polyvinylchloride (PVC)	15.3
Paper (average)	18.9	Rubber	37.2
Paper, Cardboard	18.9	Straw	19.2
Plastic (average if specifics not known)	34.9	Wood	18.4
Polycarbonate	26.9	Wool/cellulose (combined)	25.0

fuel load assessments by the proposed software provide this more accurate understanding of the actual fire risk within a specific compartment by quantifying the combustible materials present, facilitating a more reliable, dynamic, and accurate prediction of fire behavior. This approach can support improved risk management practices and decision-making, leading to more effective allocation of safety measures and training efforts. Therefore, combining real fuel load data with standardized code-based assessment can ensure that fire safety measures align with actual fire scenarios and contribute to dynamic and continuous adjustments to firefighting protocols.

4.4. Perspective on application to fire risk mapping

The distribution of fire risk can be mapped spatially, facilitating identification of fire risk regions (Huang et al., 2019). This visual representation is also an important part of fire risk assessment (Kang et al., 2025; Huang et al., 2025), which enables building users and security staff to quickly recognize areas with heightened safety vulnerability, facilitating targeted interventions and enhancing overall fire safety management (Junfeng et al., 2023; Chu et al., 2010). To this end, this work proposes a contribution toward fire risk mapping based on detected fuel locations and recognized fuel load values. It is recognized that fire risk depends not only on fuel load but also on other characteristics of the fuel and layout (e.g., flammability, proximity to heat sources, etc.). Nevertheless, mapping the fuel load spatially within a building provides an important component of this fire risk visualization.

Firstly, the fuel load recognition algorithm automatically identifies locations, categories, and fuel load values of fuels from the global-view image. The identification result of each object is a high-dimensional vector, denoting as,

$$M_i = [x_i, y_i, Q_i] \quad (15)$$

where, (x_i, y_i) is the original coordinate of the object center and Q_i is the fire risk level of each combustible category. The original coordinate of the object center is converted as the target point on the mapping plane by inverse perspective algorithms as

$$\begin{bmatrix} u_j \\ y_j \\ 1 \end{bmatrix} = \begin{bmatrix} h_{11} & h_{12} & h_{13} \\ h_{21} & h_{22} & h_{23} \\ h_{31} & h_{32} & h_{33} \end{bmatrix} \begin{bmatrix} x_j \\ y_j \\ 1 \end{bmatrix} \quad (16)$$

where, (u_i, v_i) is the transformed coordinate of the object center, h_{ij} is transformation coefficient.

Fire risk factors are classified into 5 levels, according to the characteristic fuel load values of combustible categories in the model, shown in Fig. 10(a). The categories with fuel load value less than 100 MJ are

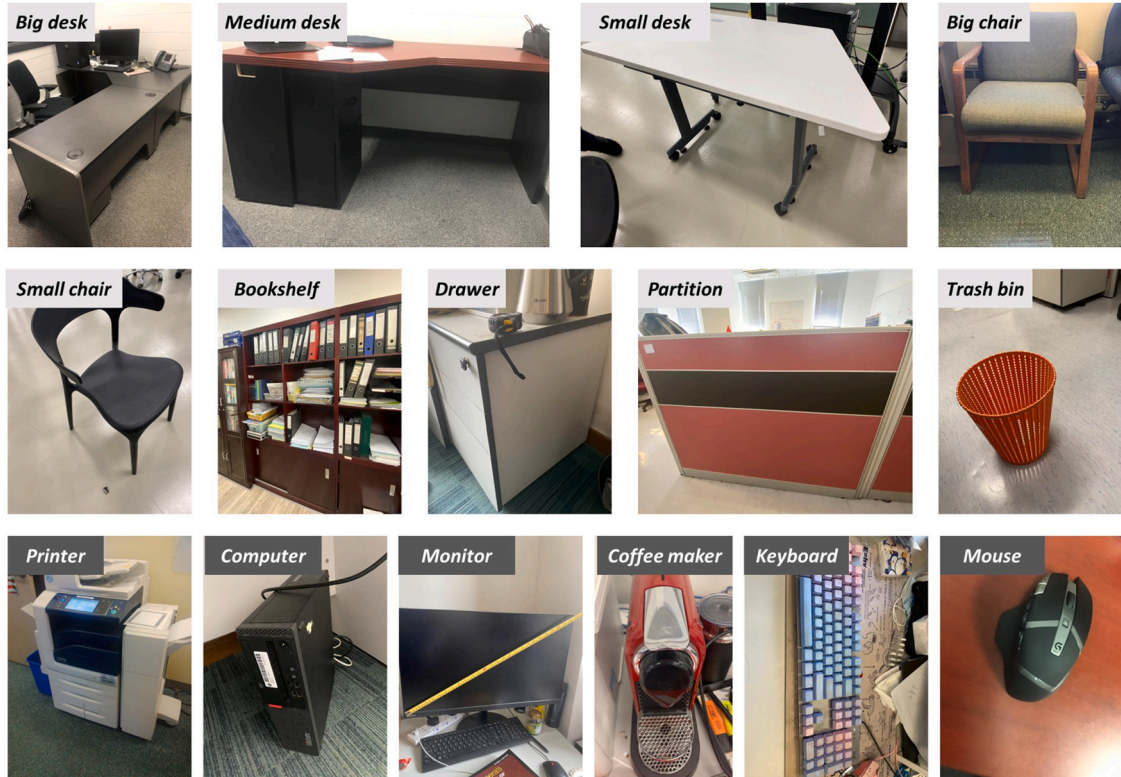


Fig. A1. Samples of different fuel categories in our custom dataset.

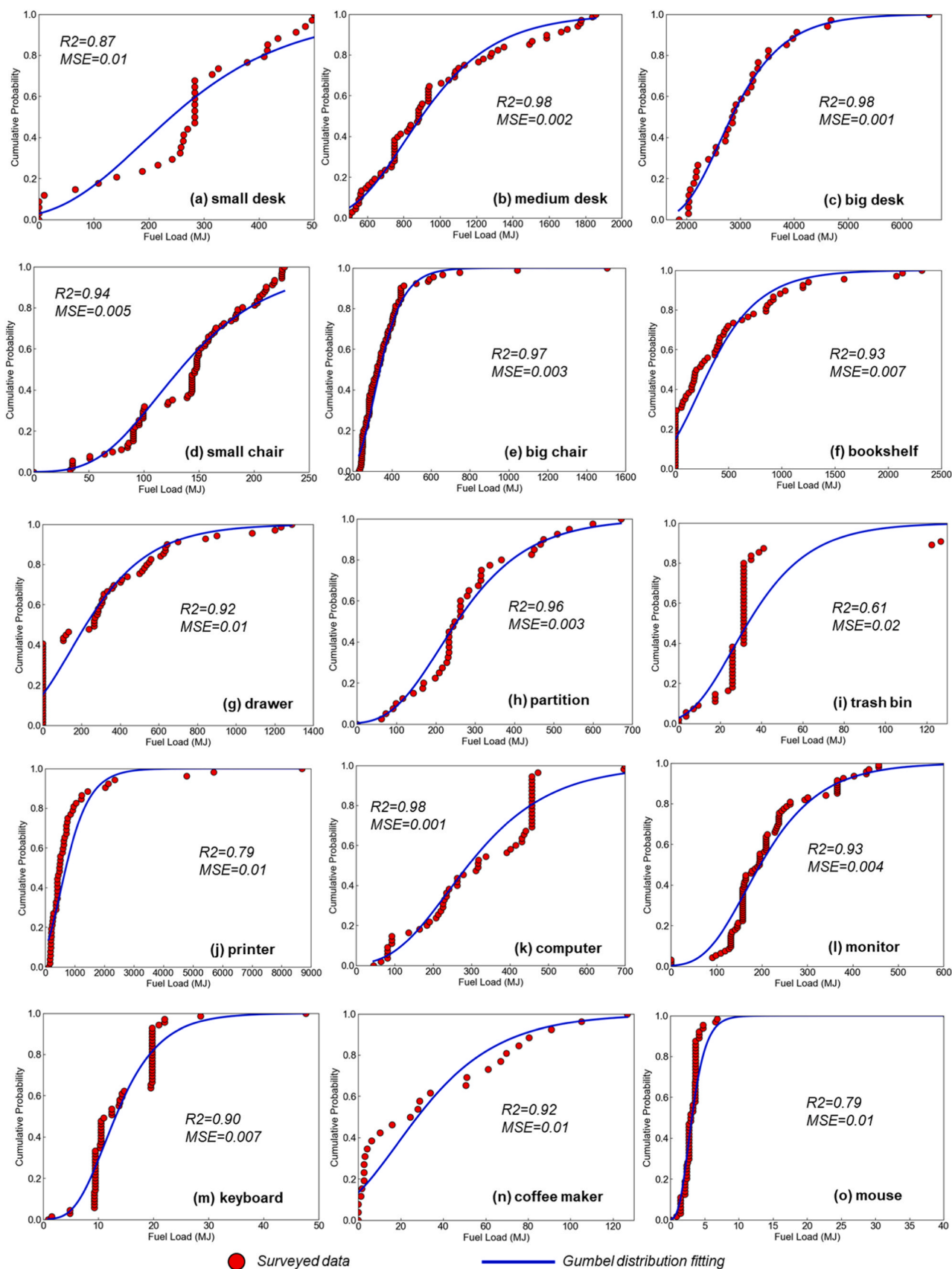


Fig. A2. Statistical and fitting results of fuel load values for different categories of fuels.

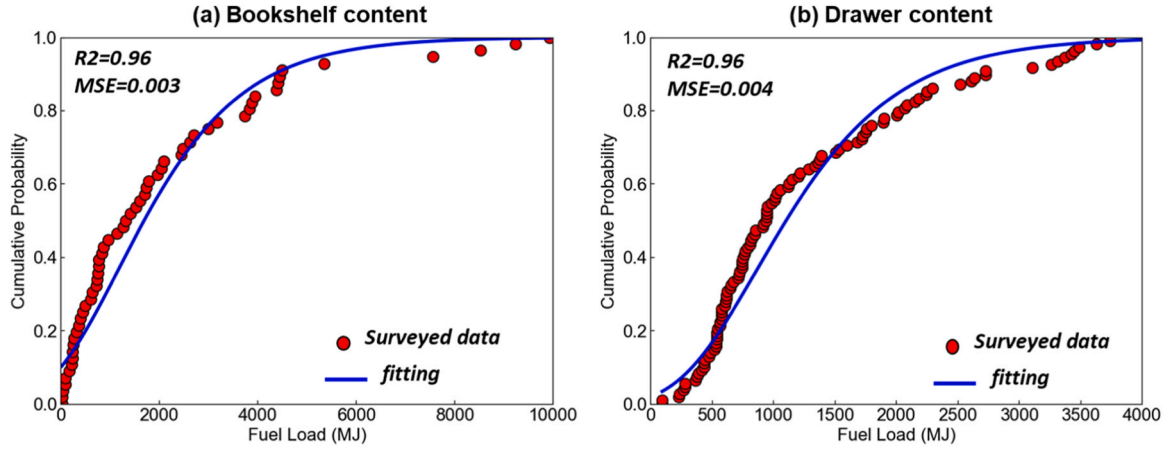


Fig. A3. Statistical and fitting results of fuel load values for (a) bookshelf content and (b) drawer content.

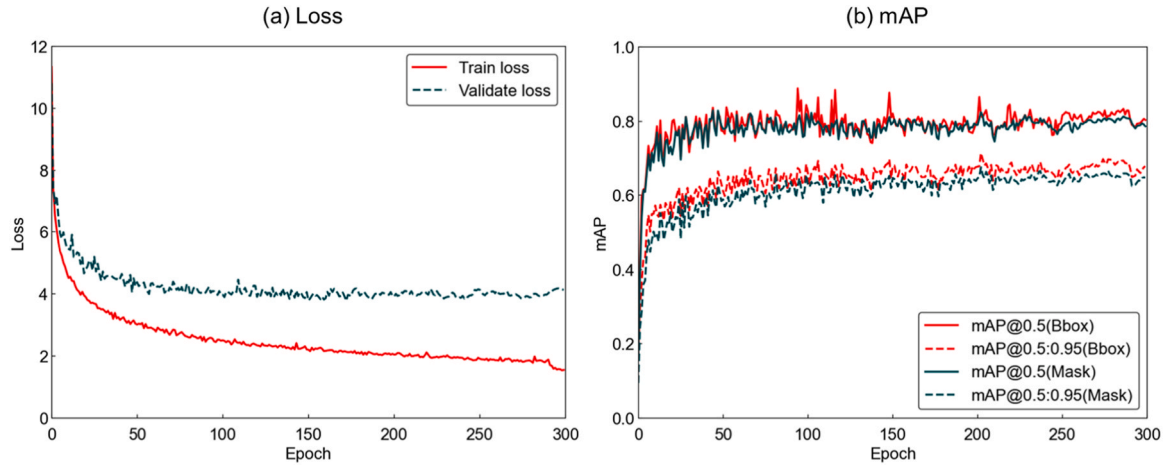


Fig. A4. Training process of YOLOv8-seg using the developed fuel dataset.

rated as “Level 1”. The categories with fuel load value ranging from 100MJ to 1000 MJ are rated as “Level 2”. The categories with fuel load value ranging from 1000 MJ to 2,000 MJ are rated as “Level 3”. The categories with fuel load value ranging from 2000MJ to 4,000 MJ are rated as “Level 4”. The categories with fuel load value larger than 4000MJ are rated as “Level 5”.

When the areas of influence of two objects overlap in the mapping frame, the risk factors in the overlapping regions are superimposed. For easier visualization, the superimposed risk factors are further standardized within the range of (0,1) as

$$R_i = \frac{Q_{\max} - Q_i}{Q_{\max} - Q_{\min}}, \quad R \in [0, 1] \quad (17)$$

The color depth ranging of (0, 255) in the heatmap is determined by the fire risk factor as.

$$C_i = R_i \times 255 \quad (18)$$

where, R_i represents the standardized risk factor, C_i represents the color of the influence area in the heatmap, Q_{\max} represents maximum risk factor after superimposition, Q_{\min} represents the minimum risk level equaling 0. The standardized risk factors are categorized as six levels: Low (0), Medium (0.25), Medium High (0.5), High (0.75), and Extreme High (1.0). The influence area is represented by a square with side length b . After that, the visualization algorithms in OpenCV and Matplotlib would be used to visualize a heat map of the risk level matrix.

Fig. 10(c) illustrates the fire risk heatmap of the demonstrated office

room under various influence areas of 0.5, 1.0 and 2.0 m. Compared to the fuel load identification in Fig. 10(b), the heatmap provides a clearer and more intuitive representation of the spatial distribution of fire risk in the room, where brighter colors indicate higher levels of danger. The visualization effects of different influence areas show that a smaller side length can more clearly illustrate the spatial distribution of various fuels. In contrast, a larger side length better demonstrates the interactions among these items and the potential spread of fire risks. Apart from the distribution of smoke and temperature and distance to exits, choosing the appropriate risk impact area for heatmap visualization allows for a comprehensive consideration of evacuation routes and the assessment of post-fire hazards.

The current risk classification method and visualization techniques for evaluating risk are crude and require further study. Additionally, the detection accuracy and generalization ability are limited by the quality and quantity of the training dataset. In future research, this method can be further developed for more accurate fire risk determination and broader application scenarios. For example, Fig. 11 illustrates the application of the fire risk mapping method in warehouse fire management, where combustibles of different fire hazards move in and out dynamically. The pre-trained AI model could detect and monitor combustibles, classifying their danger levels based on the flammability and explosivity of different goods.

The fire risk mapping module could intuitively illustrate the real-time dynamic distribution of fire risk areas, enabling warehouse personnel to easily monitor fire hazards and detect flames and smoke from self-ignition at an early stage. Moreover, it can be integrated with

digital twin technologies to enable smart fire safety management by feeding real-time CCTV video streams. Such digital twin technologies have been applied for tracking moving flames (Zhang et al., 2022b), evacuees (Ding et al., 2025), and high fire-risk vehicles in tunnels (Zhang et al., 2024b). By determining the dynamic variation of indoor fuel load distribution, potential fire incidents and the consequent fire development can be better predicted, so the emergency response can be better planned and executed.

5. Conclusions

This paper proposed an automatic fuel load and design fire methodology using a digitized fuel load database and AI technologies such as deep learning models and computer vision. An AI-aided web software was developed for rapid and real-time fuel load estimation and fire development prediction of a compartment through a user interface. The estimation method predicts the mean values and 80 fractile values of fuel load based on the fuel segmentation and classification where the overall mAP exceeds 77% in testing dataset. While the accuracy of fuel load estimations for individual components may not be high, the total fuel load based on the average values achieves sufficient accuracy, as demonstrated in an open office where the agreement between the AI method and the previously digitized survey method exceeded 94%. An important finding of the study is that the onsite estimated fuel load data tends to be higher than that used for code-based design. In line with the previous NFPA study (Elhami-Khorasani et al., 2021; Ding et al., 2024), the surveyed fuel load density from 72 rooms was found to be higher than that prescribed in the Eurocode (Institution, 2021) for the same type of occupancy. Accordingly, it results in more severe design fires, as the predicted fire duration and maximum temperature in the demonstration were higher than those derived from the code-value assessment, which may underestimate the actual fire scenario. This suggests that a revision of the code-based values of fuel load density is urgently needed. The method developed in this study can be instrumental for such revisions by enabling the efficient collection and processing of data from a large dataset of buildings.

Additionally, the proposed fire risk heatmap provided an intuitive visualization of the spatial distribution of high-load combustibles, enabling proactive measures in high-risk areas. In general, using a panoramic image of large open spaces instead of individual images of items as the input to the methodology can significantly enhance assessment efficiency. A fitted linear correlation between the fuel load within a partition and the total value of fuel load in open spaces helps mitigate the occlusion effect caused by partitions and multiple objects.

In conclusion, the AI-aided automated fuel load assessment method offers notable accessibility, convenience, and low cost while achieving satisfactory accuracy compared with the traditional methods. Furthermore, automatic design fire using actual fuel load data allows for more realistic and accurate fire behavior predictions and fire risk visualization, which leads to more effective firefighting facilities and emergency response strategies.

CRediT authorship contribution statement

Yifei Ding: Writing – original draft, Software, Methodology, Investigation, Formal analysis. **Rong Deng:** Writing – original draft, Investigation, Formal analysis. **Yuxin Zhang:** Writing – review & editing, Supervision, Formal analysis, Conceptualization. **Xinyan Huang:** Writing – review & editing, Supervision, Methodology, Funding acquisition, Conceptualization. **Negar Elhami-Khorasani:** Writing – review & editing, Formal analysis. **Thomas Gernay:** Writing – review & editing, Formal analysis.

Declaration of Competing Interest

The authors declare that they have no known competing financial

interests or personal relationships that could have appeared to influence the work reported in this paper.

Acknowledgments

The authors thank support from the Hong Kong Research Grants Council Theme-based Research Scheme (T22-505/19-N), MTR Research Fund (PTU-23005), and NFPA Fire Protection Research Foundation (FPRF).

Appendix

Table A1, Fig. A1, Fig. A2, Fig. A3, Fig. A4

Appendix A. Supporting information

Supplementary data associated with this article can be found in the online version at [doi:10.1016/j.psep.2025.107031](https://doi.org/10.1016/j.psep.2025.107031).

Data availability statement

Data will be made available on request.

References

- Barnett, C.R., 2007. Replacing international temperature–time curves with BFD curve. *Fire Saf. J.* 42, 321–327. <https://doi.org/10.1016/j.firesaf.2006.11.001>.
- Bwalya, A.C., Sultan, M.A., Bénichou, N., 2004. Institute for research in construction, National Research Council Canada Ottawa. A Pilot Surv. Fire Loads Can. Homes.
- J. Caro, T., Milke, A survey of fuel loads in contemporary office buildings, NIST GCR-96-697, National Institute of Standards and Technology, Gaithersburg, MD., (1996).
- Chu, Y., Zhang, H., Shen, S., Yang, R., Qiao, L., 2010. Development of a model to generate a risk map in a building fire. *Sci. China Technol. Sci.* 53, 2739–2747.
- Cooray, K., 2010. Generalized gumbel distribution. *J. Appl. Stat.* 37, 171–179.
- Deng, J., Dong, W., Socher, R., Li, L.-J., Li, K., Fei-Fei, L., 2009. ImageNet: a large-scale hierarchical image database. *IEEE Conf. Comput. Vis. Pattern Recognit.* 2009, 248–255. <https://doi.org/10.1109/CVPR.2009.5206848>.
- Ding, Y., Chen, X., Zhang, Y., Huang, X., 2025. Smart building evacuation by tracking multi-camera network and explainable Re-identification model. *Eng. Appl. Artif. Intell.* 148, 110394. <https://doi.org/10.1016/j.engappai.2025.110394>.
- Ding, Y., Cheung, W.K., Zhang, Y., Huang, X., 2024. Digitized fuel load survey in commercial and university office buildings for fire safety assessment. *Fire Saf. J.* 104287 <https://doi.org/10.1016/j.firesaf.2024.104287>.
- Ding, Y., Zhang, Y., Huang, X., 2023. Intelligent emergency digital twin system for monitoring building fire evacuation. *J. Build. Eng.* 77, 107416. <https://doi.org/10.1016/j.jobbe.2023.107416>.
- Dundar, U., Selamet, S., 2023. Fire load and fire growth characteristics in modern high-rise buildings. *Fire Saf. J.* 135, 103710. <https://doi.org/10.1016/j.firesaf.2022.103710>.
- Elhami-Khorasani, N., Castillo, E., Salado Saula, Juan Gustavo, Josephs, T., Nurlybekova, G., Gernay, T., 2019. Digitized fuel load survey methodology using machine vision. *Nfpa 80*. (<https://www.nfpa.org/News-and-Research/Data-research-and-tools/Building-and-Life-Safety/Digitized-Fuel-Load-Survey-Methodology-Using-Machine-Vision>).
- Elhami-Khorasani, N., Salado Castillo, J.G., Gernay, T., 2021a. A digitized fuel load surveying methodology using machine vision. *Fire Technol.* 57, 207–232. <https://doi.org/10.1007/s10694-020-00989-9>.
- Elhami-Khorasani, N., Salado Castillo, J.G., Saula, E., et al., 2021. Application of a digitized fuel load surveying methodology to office buildings. *Fire Technol.* 57, 101–122. <https://doi.org/10.1007/s10694-020-00990-2>.
- Fontana, M., Kohler, J., Fischer, K., De Sanctis, G., 2016. Fire load density. *SFPE Handb. Fire Prot. Eng.* 1131–1142.
- Gernay, T., 2019. Fire resistance and burnout resistance of reinforced concrete columns. *Fire Saf. J.* 104, 67–78. <https://doi.org/10.1016/j.firesaf.2019.01.007>.
- Her Excellency the Governor-General in Council, New Zealand, Building Regulation 1992, 2012.
- Huang, Y., Liu, D., Tang, J., Niu, S., Bell, F.M., Pena-Mora, F., 2025. Dynamic estimation of the fire service spatial accessibility for EV charging stations: Towards preventing severe fires and explosions. *Process Saf. Environ. Prot.* 195, 106734. <https://doi.org/10.1016/j.psep.2024.12.115>.
- Huang, D., Lo, S., Chen, J., Fu, Z., Zheng, Y., Luo, L., Zhuang, Y., Cheng, H., Yang, L., 2019. Mapping fire risk of passenger-carried fire load in metro system via floor field cellular automaton. *Autom. Constr.* 100, 61–72. <https://doi.org/10.1016/j.autcon.2018.12.021>.
- Huang, X., Wu, X., Usmani, A., 2022. Perspectives of using Artificial Intelligence in building fire safety. In: Naser, M.Z. (Ed.), *Handb. Cogn. Auton. Syst. Fire Resilient Infrastructures*. Springer, New York. (https://doi.org/10.1007/978-3-030-98685-8_6).

- Institution, B.S., 2021. BS EN 1991-1-2. Eurocode 1. Actions on Structures: Part 1-2. General Actions. Actions on Structures Exposed to Fire. British Standards Institution.
- Jadon, S., Kumar, S., 2025. Fire load assessment in office buildings: a comparison of survey results. *Fire Technol.* <https://doi.org/10.1007/s10694-025-01719-9>.
- Junfeng, C., Maohua, Z., Peiyun, Q., Zeng, L., Jiacheng, C., 2023. Mapping the fire risk in buildings: a hybrid method of ASET-RSET concept and FED concept. *Reliab. Eng. Syst. Saf.* 240, 109571.
- Kang, J., Su, T., Li, J., Wang, Z., Zhang, J., 2025. Research on risk evolution, prevention, and control of fire and explosion accidents in hydrogen refueling stations based on the AcciMap-FTA model. *Process Saf. Environ. Prot.* 194, 107–118. <https://doi.org/10.1016/j.psep.2024.12.033>.
- Khorasani, N.E., Garlock, M., Gardoni, P., 2014. Fire load: survey data, recent standards, and probabilistic models for office buildings. *Eng. Struct.* 58, 152–165.
- Kumar, S., Rao, C.V.S.K., 1997. Fire loads in office buildings. *J. Struct. Eng.* 123, 365–368.
- Kumari, K., Dey, P., Kumar, C., Pandit, D., Mishra, S.S., Kisku, V., Chaulya, S.K., Ray, S. K., Prasad, G.M., 2021. UMAP and LSTM based fire status and explosibility prediction for sealed-off area in underground coal mine. *Process Saf. Environ. Prot.* 146, 837–852. <https://doi.org/10.1016/j.psep.2020.12.019>.
- Li, X., Lv, C., Wang, W., Li, G., Yang, L., Yang, J., 2023. Generalized focal loss: towards efficient representation learning for dense object detection. *IEEE Trans. Pattern Anal. Mach. Intell.* 45, 3139–3153. <https://doi.org/10.1109/TPAMI.2022.3180392>.
- Liu, G., Liu, Z., Qu, G., Ren, L., Wang, L., Yan, M., 2024. Dual-agent intelligent fire detection method for large commercial spaces based on numerical databases and artificial intelligence. *Process Saf. Environ. Prot.* 191, 2485–2499. <https://doi.org/10.1016/j.psep.2024.10.010>.
- Liu, S., Qi, L., Qin, H., Shi, J., Jia, J., 2018. Path Aggregation Network for Instance Segmentation, In Proceedings of the IEEE conference on computer vision and pattern recognition 87598768.
- Ma, Z., Mäkeläinen, P., 2000. Parametric temperature–time curves of medium compartment fires for structural design. *Fire Saf. J.* 34, 361–375.
- Meyer, E.A., 2006. CSS: The Definitive Guide: The Definitive Guide. O'Reilly Media, Inc.
- A.B. MySQL, MySQL, (2001).
- National Fire Protection Association (NFPA), NFPA 557 standard for determination of fire loads for use in structural fire protection design., 2012.
- Paszke, A., Gross, S., Massa, F., Lerer, A., Bradbury, J., Chanan, G., Killeen, T., Lin, Z., Gimelshein, N., Antiga, L., 2019. Pytorch: an imperative style, high-performance deep learning library. *Adv. Neural Inf. Process. Syst.* 32.
- Shetty, N.K., Guedes Soares, C., Thoft-Christensen, P., Jensen, F.M., 1998. Fire safety assessment and optimal design of passive fire protection for offshore structures. *Reliab. Eng. Syst. Saf.* 61, 139–149. [https://doi.org/10.1016/S0951-8320\(97\)00124-5](https://doi.org/10.1016/S0951-8320(97)00124-5).
- The Building Center of Japan, The Building Standard Law of Japan August 2011, 2011.
- Torralba, A., Russell, B.C., Yuen, J., 2010. Labelme: Online image annotation and applications. *Proc. IEEE* 98, 1467–1484.
- Ultralytics, P., 2023. YOLOv, 8. Github Repos. (<https://github.com/ultralytics/ultralytics>).
- Wang, Z., Ding, Y., Zhang, T., Huang, X., 2023a. Automatic real-time fire distance, size and power measurement driven by stereo camera and deep learning. *Fire Saf. J.* 140, 103891. <https://doi.org/10.1016/j.firesaf.2023.103891>.
- Wang, Z., Zhang, T., Huang, X., 2023b. Predicting real-time fire heat release rate by flame images and deep learning. *Proc. Combust. Inst.* 39 (3), 4115–4123. <https://doi.org/10.1016/j.proci.2022.07.062>.
- Wang, Z., Zhang, T., Wu, X., Huang, X., 2022. Predicting transient building fire based on external smoke images and deep learning. *J. Build. Eng.* 47, 103823. <https://doi.org/10.1016/j.jobe.2021.103823>.
- Welling, L., Thomson, L., 2003. PHP and MySQL Web Development. Sams publishing.
- Zalok, E., Edulful, J., 2013. Assessment of fuel load survey methodologies and its impact on fire load data. *Fire Saf. J.* 62, 299–310. <https://doi.org/10.1016/j.firesaf.2013.08.011>.
- Zhang, X., Chen, X., Ding, Y., Zhang, Y., Wang, Z., Shi, J., Johansson, N., Huang, X., 2024b. Smart real-time evaluation of tunnel fire risk and evacuation safety via computer vision. *Saf. Sci.* 177, 106563.
- Zhang, T., Ding, F., Wang, Z., Xiao, F., Lu, C.X., Huang, X., 2024a. Forecasting backdraft with multimodal method: fusion of fire image and sensor data. *Eng. Appl. Artif. Intell.* 132, 107939. <https://doi.org/10.1016/j.engappai.2024.107939>.
- Zhang, Y., Huang, X., 2024. A review of tunnel fire evacuation strategies and state-of-the-art research in China. *Fire Technol.* 60, 859–892. <https://doi.org/10.1007/S10694-022-01357-5>.
- Zhang, Y.-F., Ren, W., Zhang, Z., Jia, Z., Wang, L., Tan, T., 2022a. Focal and efficient IOU loss for accurate bounding box regression. *Neurocomputing* 506, 146–157. <https://doi.org/10.1016/j.neucom.2022.07.042>.
- Zhang, T., Wang, Z., Wong, H.Y., Tam, W.C., Huang, X., Xiao, F., 2022a. Real-time forecast of compartment fire and flashover based on deep learning. *Fire Saf. J.* 130, 103579. <https://doi.org/10.1016/J.FIRESAF.2022.103579>.
- Zhang, T., Wang, Z., Zeng, Y., Wu, X., Huang, X., Xiao, F., 2022b. Building Artificial-Intelligence digital fire (AID-Fire) system: a real-scale demonstration. *J. Build. Eng.* 62, 105363. <https://doi.org/10.1016/j.jobe.2022.105363>.
- Zou, Z., Chen, K., Shi, Z., Guo, Y., Ye, J., 2023. Object detection in 20 years: a survey. *Proc. IEEE*.